Boone T, Collins F 1995 Effects of the obese gene product on body weight regulation in ob/ob mice. Science 269:540–543
15. **Halaas JL, Gajiwala KS, Maffei M, Cohen SL, Chait BT, Rabinowitz D, Lallone RL, Burley SK, Friedman JM** 1995 Weight-reducing effects of the plasma protein encoded by the obese gene. Science 269:543–546
16. **Golden PL, Maccagnan TJ, Pardridge WM** 1997 Human blood-brain barrier leptin receptor. Binding and endocytosis in isolated human brain microvessels. J Clin Invest 99:14–18
17. **Schwartz MW, Seeley RJ, Campfield LA, Burn P, Baskin DG** 1996 Identification of targets of leptin action in rat hypothalamus. J Clin Invest 98:1101–1106
18. **Satoh N, Ogawa Y, Katsuura G, Tsuji T, Masuzaki H, Hiraoka J, Okazaki T, Tamaki M, Hayase M, Yoshimasa Y, Nishi S, Hosoda K, Nakao K** 1997 Pathophysiological significance of the obese gene product, leptin, in ventromedial hypothalamus (VMH)-lesioned rats: evidence for loss of its satiety effect in VMH-lesioned rats. Endocrinology 138:947–954
19. **Farooqi IS, Bullmore E, Keogh J, Gillard J, O'Rahilly S, Fletcher PC** 2007 Leptin regulates striatal regions and human eating behavior. Science 317:1355
20. **Baicy K, London ED, Monterosso J, Wong ML, Delibasi T, Sharma A, Licinio J** 2007 Leptin replacement alters brain response to food cues in genetically leptin-deficient adults. Proc Natl Acad Sci USA 104:18276–18279
21. **Frank S, Heni M, Moss A, von Schnurbein J, Fritsche A, Häring HU, Farooqi S, Preissl H, Wabitsch M** 2011 Leptin therapy in a congenital leptin-deficient patient leads to acute and long-term changes in homeostatic, reward, and food-related brain areas. J Clin Endocrinol Metab 96:E1283–E1287
22. **Oldfield RC** 1971 The assessment and analysis of handedness: the Edinburgh inventory. Neuropsychologia 9:97–113
23. **Stoeckel LE, Kim J, Weller RE, Cox JE, Cook 3rd EW, Horwitz B** 2009 Effective connectivity of a reward network in obese women. Brain Res Bull 79:388–395
24. **Rothemund Y, Preuschhof C, Bohner G, Bauknecht HC, Klingebiel R, Flor H, Klapp BF** 2007 Differential activation of the dorsal striatum by high-calorie visual food stimuli in obese individuals. Neuroimage 37:410–421
25. **Fuhrer D, Zysset S, Stumvoll M** 2008 Brain activity in hunger and satiety: an exploratory visually stimulated FMRI study. Obesity (Silver Spring) 16:945–950
26. **Porubská K, Veit R, Preissl H, Fritsche A, Birbaumer N** 2006 Subjective feeling of appetite modulates brain activity: an fMRI study. Neuroimage 32:1273–1280
27. **Schienle A, Stark R, Walter B, Blecker C, Ott U, Kirsch P, Sammer G, Vaitl D** 2002 The insula is not specifically involved in disgust processing: an fMRI study. Neuroreport 13:2023–2026
28. **Tzourio-Mazoyer N, Landeau B, Papathanassiou D, Crivello F, Etard O, Delcroix N, Mazoyer B, Joliot M** 2002 Automated anatomical labeling of activations in SPM using a macroscopic anatomical parcellation of the MNI MRI single-subject brain. Neuroimage 15:273–289
29. **Stoeckel LE, Cox JE, Cook 3rd EW, Weller RE** 2007 Motivational state modulates the hedonic value of food images differently in men and women. Appetite 48:139–144
30. **Maldjian JA, Laurienti PJ, Kraft RA, Burdette JH** 2003 An automated method for neuroanatomic and cytoarchitectonic atlas-based interrogation of fMRI data sets. Neuroimage 19:1233–1239
31. **Lancaster JL, Woldorff MG, Parsons LM, Liotti M, Freitas CS, Rainey L, Kochunov PV, Nickerson D, Mikiten SA, Fox PT** 2000 Automated Talairach atlas labels for functional brain mapping. Hum Brain Mapp 10:120–131
32. **Siep N, Roefs A, Roebroeck A, Havermans R, Bonte ML, Jansen A** 2009 Hunger is the best spice: an fMRI study of the effects of attention, hunger and calorie content on food reward processing in the amygdala and orbitofrontal cortex. Behav Brain Res 198:149–158
33. **Chaput JP, Gilbert JA, Gregersen NT, Pedersen SD, Sjödin AM** 2010 Comparison of 150-mm versus 100-mm visual analogue scales in free living adult subjects. Appetite 54:583–586
34. **Batterham RL, ffytche DH, Rosenthal JM, Zelaya FO, Barker GJ, Withers DJ, Williams SC** 2007 PYY modulation of cortical and hypothalamic brain areas predicts feeding behaviour in humans. Nature 450:106–109
35. **Killgore WD, Yurgelun-Todd DA** 2006 Affect modulates appetite-related brain activity to images of food. Int J Eat Disord 39:357–363
36. **Zald DH, Lee JT, Fluegel KW, Pardo JV** 1998 Aversive gustatory stimulation activates limbic circuits in humans. Brain 121:1143–1154
37. **Tataranni PA, Gautier JF, Chen K, Uecker A, Bandy D, Salbe AD, Pratley RE, Lawson M, Reiman EM, Ravussin E** 1999 Neuroanatomical correlates of hunger and satiation in humans using positron emission tomography. Proc Natl Acad Sci USA 96:4569–4574
38. **Pelchat ML, Johnson A, Chan R, Valdez J, Ragland JD** 2004 Images of desire: food-craving activation during fMRI. Neuroimage 23:1486–1493
39. **Morris JS, Dolan RJ** 2001 Involvement of human amygdala and orbitofrontal cortex in hunger-enhanced memory for food stimuli. J Neurosci 21:5304–5310
40. **O'Doherty JP, Deichmann R, Critchley HD, Dolan RJ** 2002 Neural responses during anticipation of a primary taste reward. Neuron 33:815–826

Intracerebroventricular Administration of C-Type Natriuretic Peptide Suppresses Food Intake via Activation of the Melanocortin System in Mice

Nobuko Yamada-Goto,[1] Goro Katsuura,[1] Ken Ebihara,[1] Megumi Inuzuka,[1] Yukari Ochi,[1] Yui Yamashita,[1] Toru Kusakabe,[1] Akihiro Yasoda,[1] Noriko Satoh-Asahara,[2] Hiroyuki Ariyasu,[1] Kiminori Hosoda,[1] and Kazuwa Nakao[1]

C-type natriuretic peptide (CNP) and its receptor are abundantly distributed in the brain, especially in the arcuate nucleus (ARC) of the hypothalamus associated with regulating energy homeostasis. To elucidate the possible involvement of CNP in energy regulation, we examined the effects of intracerebroventricular administration of CNP on food intake in mice. The intracerebroventricular administration of CNP-22 and CNP-53 significantly suppressed food intake on 4-h refeeding after 48-h fasting. Next, intracerebroventricular administration of CNP-22 and CNP-53 significantly decreased nocturnal food intake. The increment of food intake induced by neuropeptide Y and ghrelin was markedly suppressed by intracerebroventricular administration of CNP-22 and CNP-53. When SHU9119, an antagonist for melanocortin-3 and melanocortin-4 receptors, was coadministered with CNP-53, the suppressive effect of CNP-53 on refeeding after 48-h fasting was significantly attenuated by SHU9119. Immunohistochemical analysis revealed that intracerebroventricular administration of CNP-53 markedly increased the number of c-Fos–positive cells in the ARC, paraventricular nucleus, dorsomedial hypothalamus, ventromedial hypothalamic nucleus, and lateral hypothalamus. In particular, c-Fos–positive cells in the ARC after intracerebroventricular administration of CNP-53 were coexpressed with α-melanocyte–stimulating hormone immunoreactivity. These results indicated that intracerebroventricular administration of CNP induces an anorexigenic action, in part, via activation of the melanocortin system.

C-type natriuretic peptide (CNP) is a member of the natriuretic peptide family and has been demonstrated to be abundantly present in the brain, interestingly in discrete hypothalamic areas, such as the arcuate nucleus (ARC) of the hypothalamus, that play pivotal roles in energy regulation (1–3). Two predominant molecular forms of CNP in the porcine brain were reported to be a 22-residue peptide (CNP-22) and its *N*-terminally elongated 53-residue peptide (CNP-53) (1). Moreover, natriuretic peptide receptor-B (NPR-B), a CNP receptor, also is widely distributed in the brain and is reported to be abundantly expressed in the ARC of the hypothalamus (4,5). These findings indicate the possibility that the brain CNP/NPR-B system may regulate energy homeostasis.

In the current study, we examined the effects of intracerebroventricular administration of CNP on food intake induced by refeeding after fasting and by orexigenic peptides, such as neuropeptide Y (NPY) and ghrelin. Also, we examined the involvement of the melanocortin system in the CNP actions.

RESEARCH DESIGN AND METHODS

Animals and diets. Male C57BL/6J mice (6 weeks old) obtained from Japan SLC (Shizuoka, Japan) were housed in plastic cages in a room kept at a room temperature of 23 ± 1°C and a 12:12-h light–dark cycle (lights turned on at 9:00 A.M.). The mice had ad libitum access to water and food (CE-2; CLEA Japan, Tokyo, Japan). All experiments were performed at 10 weeks of age in accordance with the guidelines established by the Institutional Animal Investigation Committee at Kyoto University and the United States National Institutes of Health Guide for the Care and Use of Laboratory Animals. Every effort was made to optimize comfort and to minimize the use of animals.

Peptides. CNP-22, CNP-53, ghrelin, and NPY were purchased from Peptide Institute (Osaka, Japan). SHU9119 was purchased from Bachem AG (Bubendorf, Switzerland).

Intracerebroventricular injection. Intracerebroventricular injection was performed according to our previous report (6).

Measurement of food intake

Fasting-refeeding. Mice were fasted for 48 h and then refed for 4 h. Water was available ad libitum during the experiments. The intracerebroventricular or intraperitoneal administration of CNP-22 or CNP-53 was performed just before refeeding. Food intake was measured for 4 h of refeeding. At the end of experiments, the hypothalamus was collected for examination of the expressions of mRNA for neuropeptides (7).

Nocturnal food intake. To assess the effect of intracerebroventricular administration of CNP-22 or CNP-53 on nocturnal food intake, peptides were injected intracerebroventricularly 1 h before the beginning of the dark phase. Food intake was measured for 15 h after intracerebroventricular injection. Water was available ad libitum during the experiments.

Food intake induced by NPY and ghrelin. The experiments were performed from 11:00 A.M. to 3:00 P.M. CNP-22 or CNP-53 was intracerebroventricularly administrated just before intracerebroventricular injection of NPY (5 nmol/mouse) or intraperitoneal injection of ghrelin (100 nmol/kg). Food intake was measured for 4 h after peptide injection. In these experiments, food and water were available ad libitum.

PCR. The extraction of mRNA and quantitative real-time RT-PCR were performed according to our previous report (8). Primers for *preopiomelanocortin, cocaine and amphetamine-related peptide, NPY, agouti gene-related peptide (AgRP)* and *glyceraldehyde 3-phosphate dehydrogenase* are shown in Supplementary Table 1.

Immunohistochemistry for c-Fos and α-MSH in the hypothalamus. The immunohistochemical methods and the stereotaxic coordinates for the hypothalamic nuclei were based on our previous report (6). Briefly, mice were anesthetized with pentobarbital at 1 h after intracerebroventricular injection of CNP-53 (1.5 nmol/mouse) and perfused with 50 mL 0.1 mol/L PBS, followed by 50 mL ice-cold 4% paraformaldehyde in 0.1 mol/L PBS. Sections of 30-μm thickness were cut with a cryostat. According to the mouse brain atlas (9), cross-sections were selected in correspondence to −1.70 mm [ARC, lateral hypothalamus (LH), dorsomedial hypothalamus (DMH), ventromedial hypothalamic

From the [1]Department of Medicine and Clinical Science, Kyoto University Graduate School of Medicine, Kyoto, Japan; and the [2]Clinical Research Institute, National Hospital Organization, Kyoto Medical Center, Kyoto, Japan.
Corresponding author: Nobuko Yamada-Goto, nobukito@kuhp.kyoto-u.ac.jp.
Received 31 May 2012 and accepted 7 November 2012.
DOI: 10.2337/db12-0718
This article contains Supplementary Data online at http://diabetes.diabetesjournals.org/lookup/suppl/doi:10.2337/db12-0718/-/DC1.

See accompanying commentary, p. XXX.

nucleus (VMH)] and to −0.82 mm [paraventricular nucleus (PVN)], relative to bregma. For c-Fos and α-melanocyte–stimulating hormone (α-MSH) protein staining, the sections were incubated with antic-Fos rabbit antibody (Ab-5; 1:5,000; Oncogene Science, Cambridge, MA) and antiα-MSH sheep antibody (AB5087; 1:10,000; EMD Millipore, Billerica, MA), respectively. The antibody was detected using the Vectastain ABC Elite kit (PK-6101; Vector Laboratories, Burlingame, CA) and a diaminobenzidine substrate kit (SK-4100; Vector Laboratories) was used for visualization. The second antibodies for fluorescence visualization used were goat anti-rabbit488 (A11008; 1:200; Life Technologies, Carlsbad, CA) for antic-Fos rabbit antibody and goat anti-sheep546 (A21098; 1:200; Life Technologies) for antiα-MSH sheep antibody.

Data analysis. All values are given as the mean ± SEM. Statistical analysis of the data were performed by ANOVA, followed by the Tukey-Kramer test. Statistical significance was defined as $P < 0.05$.

RESULTS

Effects of intracerebroventricular administration of CNP-22 and CNP-53 on food intake at refeeding after fasting. The intracerebroventricular administration of CNP-22 (1.5 and 4.5 nmol/mouse) and CNP-53 (1.5 nmol/mouse) significantly suppressed food intake during 4-h refeeding after 48-h fasting in comparison with data from saline-treated mice (Fig. 1*A*). In this experiment, CNP-53 (1.5 nmol), but not other treatments, induced significant reduction of body weight compared with saline treatment (Supplementary Table 2). The mRNA expressions of *pre-opiomelanocortin* and *cocaine and amphetamine-related peptide* significantly decreased, and the mRNA expressions of *NPY* and *AgRP* significantly increased after refeeding compared with control animals (Supplementary Fig. 1). The intracerebroventricular administration of CNP-53 did not influence the mRNA expressions of these neuropeptides in the hypothalamus (Supplementary Fig. 1). Next, the peripheral action of CNP on food intake was examined when a 10-fold greater dose than intracerebroventricular injection of each CNP was intraperitoneally administered. The intraperitoneal administrations of CNP-22 (1.5 μmol/kg) and CNP-53 (0.5 μmol/kg) did not change the food intake during 4-h refeeding after 48-h fasting (Fig. 1*B*), nor were there changes in body weight (Supplementary Table 3).

The intracerebroventricular administrations of CNP-22 (4.5 nmol/mouse) and CNP-53 (1.5 nmol/mouse) at 1 h before the start of the dark phase significantly suppressed nocturnal food intake compared with saline treatment (Fig. 1*C*).

Effect of intracerebroventricular administration of CNP-22 and CNP-53 on NPY-induced and ghrelin-induced food intake. When CNP-22 (4.5 nmol/mouse) and CNP-53 (1.5 nmol/mouse) were concomitantly administered intracerebroventricularly with NPY, they significantly suppressed the food intake induced by NPY compared with that of saline treatment (Fig. 2*A*). When CNP-22 (4.5 nmol/mouse) and CNP-53 (1.5 nmol/mouse) were administered intracerebroventricularly with ghrelin, they significantly suppressed the food intake induced by ghrelin compared with that of saline treatment (Fig. 2*B*).

Effect of melanocortin receptor antagonist, SHU9119, on the anorectic effect of CNP. To examine its involvement in the anorectic effect of CNP, SHU9119 was administered intracerebroventricularly together with CNP-53 (1.5 nmol/mouse). SHU9119 (1 nmol/mouse) significantly attenuated the suppressive action of CNP-53 on the food intake during 4-h refeeding after 48-h fasting, whereas SHU9119 itself significantly enhanced the increase of food intake in comparison with mice administered saline treatment (Fig. 3).

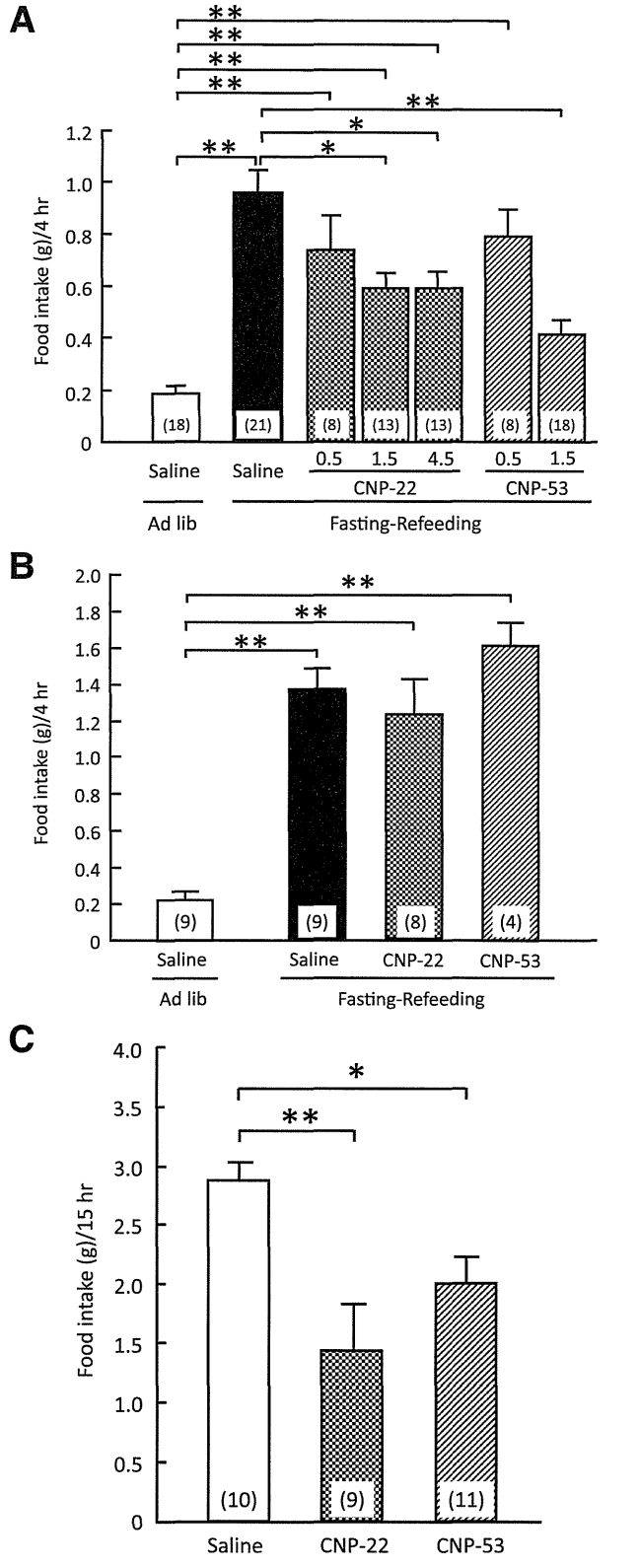

FIG. 1. Effects of CNP on refeeding after fasting. *A*: Effects of intracerebroventricular administration of CNP-22 (0.5, 1.5, and 4.5 nmol/mouse) and CNP-53 (0.5 and 1.5 nmol/mouse) on 4-h refeeding after 48-h fasting in mice. Food intake was observed for 4 h after refeeding. *B*: Effects of intraperitoneal administration of CNP-22 (1.5 μmol/kg) and CNP-53 (0.5 μmol/kg) on 4-h refeeding after 48-h fasting in mice. Food intake was observed for 4 h after refeeding. *C*: Effects of intracerebroventricular administration of CNP-22 (4.5 nmol/mouse) and CNP-53 (1.5 nmol/mouse) on nocturnal food intake in mice. Food intake was observed for 15 h after intracerebroventricular injection. Data represent mean ± SEM. The number of mice is given in parentheses. Significant differences: *$P < 0.05$, **$P < 0.01$.

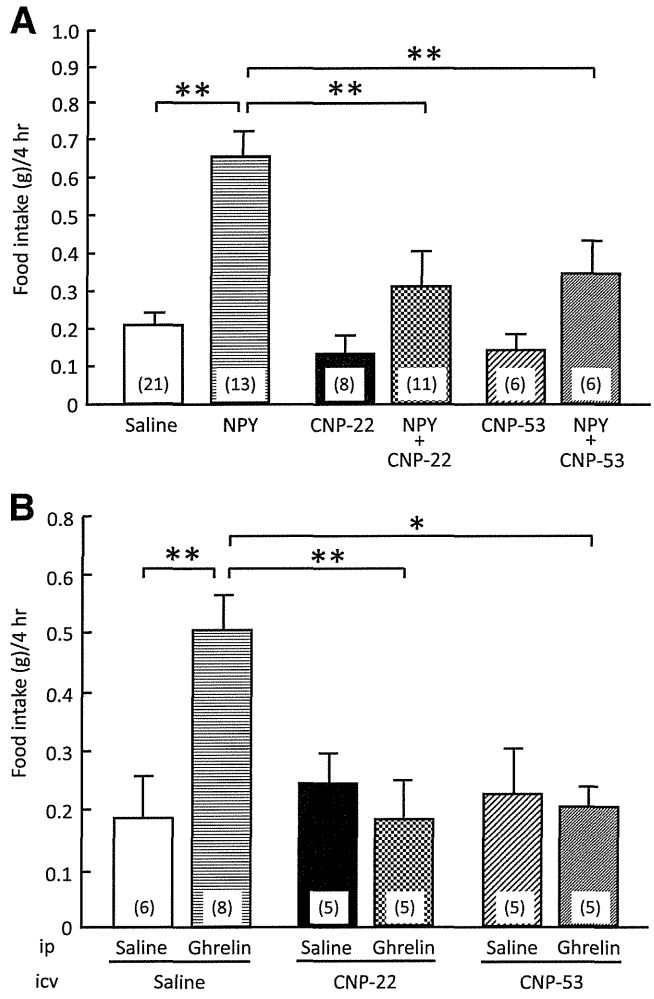

FIG. 2. Effects of CNP-22 and CNP-53 on food intake induced by NPY and ghrelin. *A*: Effects of intracerebroventricular administration of CNP-22 (4.5 nmol/mouse) and CNP-53 (1.5 nmol/mouse) on NPY-induced (5 nmol/mouse, intracerebroventricular) food intake in mice. Food intake was observed for 4 h after coadministration of NPY and CNP. *B*: Effects of intracerebroventricular administration of CNP-22 (4.5 nmol/mouse) and CNP-53 (1.5 nmol/mouse) on ghrelin-induced (100 nmol/kg, intraperitoneal) food intake in mice. Food intake was observed for 4 h after coadministration of ghrelin and CNP. Data represent mean ± SEM. The number of mice is given in parentheses. Significant differences: *$P < 0.05$, **$P < 0.01$.

c-Fos–immunoreactive cells in the hypothalamus after intracerebroventricular administration of CNP. To understand the neuronal pathway involved in the anorectic actions of CNP, the expression of c-Fos, one of the markers of neuronal activation, was monitored by immunohistochemical examination at 1 h after intracerebroventricular injection of CNP-53 (1.5 nmol/mouse). The numbers of c-Fos–immunoreactive cells in the ARC, PVN, and DMH were predominantly increased after intracerebroventricular injection of CNP-53 in comparison with saline treatment (Fig. 4*A*). The c-Fos–positive cells also were moderately increased in the VMH and LH (Fig. 4*A*). Next, we examined whether c-Fos immunoreactivity coexisted with α-MSH–containing cells. In the ARC of saline-treated mice, only a few α-MSH–immunoreactive cells showed weak c-Fos immunoreactivity (Fig. 4*B*). However, c-Fos–immunoreactive cells that increased with intracerebroventricular administration of CNP-53 in the ARC expressed a large amount of α-MSH immunoreactivity (Fig. 4*B*).

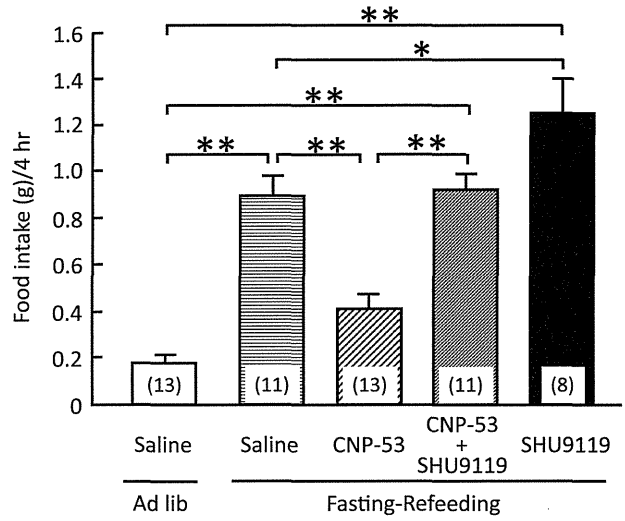

FIG. 3. Effects of intracerebroventricular administration of CNP-53 (1.5 nmol/mouse) and SHU9119 (1 nmol/mouse) on refeeding after 48-h fasting in mice. Food intake was observed for 4 h after refeeding. Data represent mean ± SEM. The number of mice is given in parentheses. Significant differences: *$P < 0.05$, **$P < 0.01$.

DISCUSSION

The current study demonstrated that intracerebroventricular administration of CNP-22 and CNP-53, but not intraperitoneal injection, led to significant reduction of food intake induced by fasting–refeeding. This reduction was inhibited by the melanocortin-3 receptor (MC3R)/melanocortin-4 receptor (MC4R) antagonist SHU9119. In addition, CNP significantly suppressed nocturnal food intake and orexigenic actions induced by NPY and ghrelin. The immunohistochemical study revealed that intracerebroventricular administration of CNP-53 increased the number of c-Fos–expressing cells containing α-MSH in the hypothalamus. These findings indicated that the intracerebroventricular administration of CNP exhibits anorexigenic actions partially via activation of the melanocortin system, although the doses of CNP used in the current study could be pharmacological doses.

The hypothalamus is considered to be an important region in regulating energy homeostasis. In particular, the ARC in the hypothalamus contains both an orexigenic peptide, NPY, and an anorexigenic peptide, α-MSH, and is postulated to be involved in the first-order regulation of food intake. Synthetic MC3R/MC4R agonists, melanotan II, and [Nle^4-D-Phe^7]–α-MSH completely blocked food deprivation–induced increase in food intake as well as the food intake stimulated by intracerebroventricular administration of NPY (10,11). Regarding the reciprocal interactions of α-MSH and NPY, melanocortin neurons in the ARC project to the PVN (12). In the current study, intracerebroventricular administration of CNP significantly suppressed food intake after fasting, which was antagonized by SHU9119. Our results also showed that CNP suppressed NPY-induced food intake. Taken together, these findings indicate that CNP exhibits anorexigenic actions via activation of MC3R/MC4R downstream signaling. However, mRNA expressions of *preopiomelanocortin, cocaine and amphetamine-related peptide*, *NPY*, and *AgRP* in the hypothalamus after the intracerebroventricular injection of CNP-53 in fasting–refeeding experiment did not change compared with those after saline. The reason for this

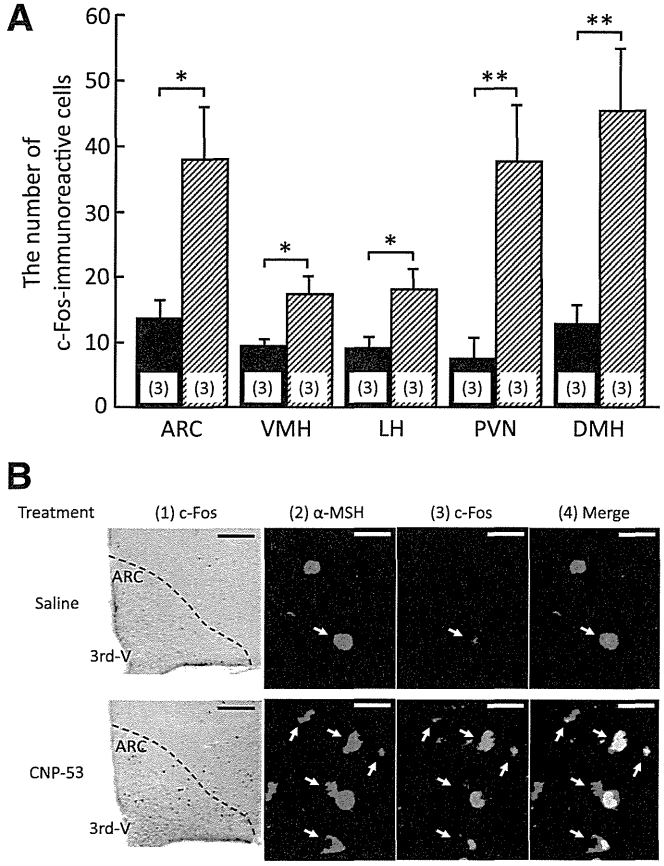

FIG. 4. The c-Fos–immunoreactive cells in the hypothalamus after intracerebroventricular administration of CNP-53 (1.5 nmol/mouse). *A*: Number of c-Fos–immunoreactive cells after saline and CNP-53 treatments. Data represent mean ± SEM. The number of mice is given in parentheses. Significant differences: *$P < 0.05$, **$P < 0.01$. *B*: c-Fos–immunoreactive cells induced by intracerebroventricular administration of saline and CNP-53 (*1*). 3rd-V, the third ventricular. Scale bars, 100 μm. Coexistence of α-MSH (*red*) and c-Fos (*green*) immunoreactivity in the ARC (*2–4*) after saline (*upper*) and CNP-53 (1.5 nmol/mouse; *lower*) treatments. *White arrows* indicate cells expressing both α-MSH and c-Fos immunoreactivity. 3rd-V, the third ventricular. Scale bars, 20 μm.

discrepancy may lie in the experimental condition, time course, and regional specificity. To clarify this discrepancy, further examinations will be required.

This study demonstrated that the intracerebroventricular administration of CNP significantly suppressed the nocturnal food intake. Robust feeding during the nocturnal phase of the daily light–dark cycle was demonstrated to be attributed to the upregulation of NPY and its receptors (13). These findings indicate that CNP may decrease food intake in the nocturnal phase via suppression of NPY action.

In the current study, CNP significantly suppressed the increase in food intake induced by ghrelin, an orexigenic hormone secreted by the stomach (14). NPR-B, a CNP receptor, has been identified in appetite-regulating regions, such as the ARC, VMH, PVN, DMH, and LH (15). The systemic administration of ghrelin significantly increased NPY and AgRP expression in the ARC of the hypothalamus in fed and fasted rats (15), resulting in hyperphagia. The intracerebroventricular injection of melanotan II caused a significant decrease in ghrelin-induced food intake (16). These findings suggest that the actions of ghrelin are modulated by α-MSH and NPY systems. Furthermore, plasma ghrelin and hypothalamic *ghrelin receptor* mRNA expression are reported to be increased after fasting (17,18). These findings suggest the possibility that intracerebroventricular administration of CNP activates the melanocortin system, which subsequently inhibits the action of NPY, resulting in a reduced increase of food intake induced by ghrelin.

To assess which hypothalamic nucleus is involved in the anorexigenic action of CNP, a marker for neuronal activity, c-Fos expression in the hypothalamus was examined after intracerebroventricular administration of CNP-53. The intracerebroventricular administration of CNP-53 significantly increased the number of c-Fos–expressing cells in several hypothalamic nuclei, such as ARC, PVN, DMH, VMH, and LH, indicating that CNP-53 directly or indirectly stimulates neurons in these hypothalamic nuclei. Especially in the ARC, the result was an increased number of c-Fos–immunoreactive cells containing α-MSH immunoreactivity, indicating that CNP stimulates α-MSH–containing neurons. This possibility is supported by the finding that the suppressive action of CNP-53 on food intake was blocked by concomitant administration of SHU9119, an MC3R/MC4R antagonist.

The current study has demonstrated the anorexigenic action of intracerebroventricular administration of CNP via activation of the melanocortin system. To define the precise effect of CNP in the brain on food intake, further investigation using mice with inducible brain-specific deletion of CNP or NPR-B/NPR-C will be required.

From the present findings, we postulate the possible mechanism for anorexigenic action of exogenous CNP to be as follows: CNP directly or indirectly acts on α-MSH–containing neurons and subsequently stimulates α-MSH release, resulting in suppression of food intake induced by NPY and ghrelin. This possible mechanism may apply to the suppressive effects of CNP on food intake after fasting and in the nocturnal phase. Further work is needed to define the pathophysiological significance of brain CNP in regulation of food intake.

ACKNOWLEDGMENTS

This work was supported in part by research grants from the Ministry of Education, Culture, Sports, Science, and Technology of Japan, the Ministry of Health, Labour, and Welfare of Japan.

No potential conflicts of interest relevant to this article were reported for N.Y.-G., G.K., K.E., M.I., Y.O., Y.Y., T.K., A.Y., N.S-A., H.A., K.H., and K.N.

N.Y.-G. and G.K. performed experiments, contributed to discussion, and wrote the manuscript. K.E., M.I., Y.O., Y.Y., T.K., A.Y., N.S.-A., H.A., and K.H. contributed to discussion. K.N. contributed to discussion, and reviewed and edited the manuscript. K.N. is the guarantor of this work and, as such, had full access to all the data in the study and takes responsibility for the integrity of the data and the accuracy of the data analysis.

REFERENCES

1. Minamino N, Makino Y, Tateyama H, Kangawa K, Matsuo H. Characterization of immunoreactive human C-type natriuretic peptide in brain and heart. Biochem Biophys Res Commun 1991;179:535–542
2. Herman JP, Langub MC Jr, Watson RE Jr. Localization of C-type natriuretic peptide mRNA in rat hypothalamus. Endocrinology 1993;133:1903–1906
3. Langub MC Jr, Watson RE Jr, Herman JP. Distribution of natriuretic peptide precursor mRNAs in the rat brain. J Comp Neurol 1995;356:183–199
4. Langub MC Jr, Dolgas CM, Watson RE Jr, Herman JP. The C-type natriuretic peptide receptor is the predominant natriuretic peptide receptor mRNA expressed in rat hypothalamus. J Neuroendocrinol 1995;7:305–309

5. Herman JP, Dolgas CM, Rucker D, Langub MC Jr. Localization of natriuretic peptide-activated guanylate cyclase mRNAs in the rat brain. J Comp Neurol 1996;369:165-187
6. Yamada N, Katsuura G, Ochi Y, Ebihara K, Kusakabe T, Hosoda K, Nakao K. Impaired CNS leptin action is implicated in depression associated with obesity. Endocrinology 2011;152:2634–2643
7. Nakao K, Katsuura G, Morii N, Itoh H, Shiono S, Yamada T, Sugawara A, Sakamoto M, Saito Y, Eigyo M, Matsushita A, Imura H. Inhibitory effect of centrally administered atrial natriuretic polypeptide on the brain dopaminergic system in rats. Eur J Pharmacol 1986;131:171–177
8. Yamada N, Katsuura G, Tatsuno I, et al. Orexin decreases mRNA expressions of NMDA and AMPA receptor subunits in rat primary neuron cultures. Peptides 2008;29:1582–1587
9. Paxinos G, Franklin KBJ. *The mouse brain in stereotaxic coordinates.* New York, Academic Press, 2004
10. Brown KS, Gentry RM, Rowland NE. Central injection in rats of alpha-melanocyte-stimulating hormone analog: effects on food intake and brain Fos. Regul Pept 1998;78:89–94
11. Murphy B, Nunes CN, Ronan JJ, et al. Melanocortin mediated inhibition of feeding behavior in rats. Neuropeptides 1998;32:491–497
12. Sánchez E, Singru PS, Acharya R, et al. Differential effects of refeeding on melanocortin-responsive neurons in the hypothalamic paraventricular nucleus. Endocrinology 2008;149:4329–4335
13. Kalra PS, Dube MG, Xu B, Farmerie WG, Kalra SP. Evidence that dark-phase hyperphagia induced by neurotoxin 6-hydroxydopamine may be due to decreased leptin and increased neuropeptide Y signaling. Physiol Behav 1998;63:829–835
14. Kojima M, Hosoda H, Date Y, Nakazato M, Matsuo H, Kangawa K. Ghrelin is a growth-hormone-releasing acylated peptide from stomach. Nature 1999;402:656–660
15. Harrold JA, Dovey T, Cai XJ, Halford JC, Pinkney J. Autoradiographic analysis of ghrelin receptors in the rat hypothalamus. Brain Res 2008;1196:59–64
16. Shrestha YB, Wickwire K, Giraudo SQ. Action of MT-II on ghrelin-induced feeding in the paraventricular nucleus of the hypothalamus. Neuroreport 2004;15:1365–1367
17. Keen-Rhinehart E, Bartness TJ. NPY Y1 receptor is involved in ghrelin- and fasting-induced increases in foraging, food hoarding, and food intake. Am J Physiol Regul Integr Comp Physiol 2007;292:R1728–R1737
18. Kim MS, Yoon CY, Park KH, et al. Changes in ghrelin and ghrelin receptor expression according to feeding status. Neuroreport 2003;14:1317–1320

CHAPTER TEN

Enzymatic Characterization of GOAT, ghrelin *O*-acyltransferase

Hideko Ohgusu, Tomoko Takahashi, Masayasu Kojima[1]
Molecular Genetics, Institute of Life Science, Kurume University, Kurume, Fukuoka, Japan
[1]Corresponding author: e-mail address: kojima_masayasu@kurume-u.ac.jp

Contents

Abstract

Ghrelin is a gastric peptide hormone in which serine 3 (threonine 3 in frogs) is modified primarily by an *n*-octanoic acid; this modification is essential for ghrelin's activity. The enzyme that transfers *n*-octanoic acid to the third serine residue of ghrelin peptide has been identified and named GOAT for ghrelin *O*-acyltransferase. GOAT is the only known enzyme that catalyzes the acyl modification of ghrelin and specifically modifies the third amino acid serine and does not modify other serine residues in ghrelin peptides. GOAT prefers *n*-hexanoyl-CoA over *n*-octanoyl-CoA as the acyl donor, although in the stomach *n*-octanoyl form is the main acyl-modified ghrelin and the concentration of *n*-hexanoyl form is very low. Moreover, a four-amino acid peptide derived from the N-terminal sequence of ghrelin can be modified by GOAT, indicating that these four amino acids constitute the core motif for substrate recognition by the enzyme.

Methods in Enzymology, Volume 514
ISSN 0076-6879
http://dx.doi.org/10.1016/B978-0-12-381272-8.00010-6

1. INTRODUCTION

Ghrelin is identified in almost all mammalian and nonmammalian vertebrate species, including frogs, birds, and fish (Kojima and Kangawa, 2005). A characteristic feature of ghrelin is an acyl modification at the third amino acid, which is typically serine or threonine. This acyl modification is necessary for ghrelin to bind to its receptor, namely, the GHS-R, and exert biological activity (Kojima et al., 1999). The structure of ghrelin, particularly that of the acyl-modification region, is highly conserved throughout all vertebrate species (Kojima et al., 2008). The primary fatty acid that acylates ghrelin is *n*-octanoic acid. However, the mechanism underlying this unique modification is still unknown. Thus, investigations characterizing the putative ghrelin ser *O*-acyltransferase are needed.

In 1998, Yang et al. reported that the membrane-bound acyltransferase MBOAT4 is a ghrelin *O*-acyltransferase (GOAT) that catalyzes *n*-octanoyl modifications of ghrelin in cultured cells (Yang et al., 2008). The observation that GOAT knockout mice lacked octanoylated ghrelin confirmed the role of GOAT in this process (Gutierrez et al., 2008). Using a combination of recombinant GOAT and ghrelin-specific immunoassays, we showed that GOAT catalyzes the *n*-octanoyl modification of ghrelin *in vitro* (Ohgusu et al., 2009). With this platform in hand, we analyzed the basic enzymatic characteristics such as the optimal temperature and pH, and profiled the peptide and acyl substrate specificities of GOAT.

2. GOAT ENZYMATIC ASSAY

2.1. Construction of stable GOAT-expressing cells and preparation of GOAT

To characterize GOAT enzymatic activity, we first established a stable GOAT-expressing cell line and prepared the enzyme from the cell cultures (Ohgusu et al., 2009).

1. Primer pairs were designed on the basis of the cDNA sequence of mouse GOAT (GenBank accesssion No. EU721729). The primer sequences were sense 5′-TCAAGCTTAGGATGGATTGGCTCCAGCTCTTTTTTC TGCATCCTTTATC-3′ and antisense 5′-GACTCGAGTCAGTTAC GTTTGTCTTTTCTCTCCGCTAACAG-3′, containing a HindIII and a XhoI site, respectively.

2. Mouse GOAT cDNA was amplified by PCR from stomach cDNA using Pyrobest DNA polymerase (Takara Bio Inc., Ohtsu, Japan).
3. The amplified cDNA fragment was inserted into a pcDNA3.1 vector at the HindIII-XhoI site.
4. CHO cells were transfected with the GOAT-pcDNA3.1 vector using Lipofectamine 2000 reagent (Invitrogen, Carlsbad, CA) and cultured in α-MEM medium with G418 (1 mg/ml) for stable cell selection.
5. Cells that grew in the presence of G418 were tested for expression of GOAT mRNA by PCR. The primers used were the same as those employed for amplifying GOAT cDNA (Step 1). The cell with the highest GOAT expression level was used for the following experiments.
6. GOAT-expressing CHO cells were cultured to 80–90% confluence in 12 100-mm culture plates (IWAKI, Tokyo, Japan). Then, the cells were homogenized by a Teflon homogenizer in the extraction buffer: 100 m*M* Tris–HCl (pH 7.4) containing 1 m*M* PMSF (phenylmethylsulfonyl fluoride), 0.8 n*M* aprotinin, 15 μ*M* E-64, 20 μM leupeptin, 50 μ*M* bestatin, and 10 μ*M* pepstatin A.
7. First, the homogenate was centrifuged at 800 × *g* for 5 min. Then, the resultant supernatant was further centrifuged at 100,000 × *g* for 1 h. The pellet was dissolved in the same extraction buffer and stored at −80 °C. The described subcellular fractionation procedure provided specific ghrelin *n*-octanoyl transferase activity in the 100,000 × *g* pellet but not the supernatant (Fig. 10.1). These results indicated that GOAT was a membrane-bound enzyme. In addition, control CHO cells demonstrated no GOAT activity (Fig. 10.1). We looked for GOAT activity in preparations of mouse stomach membrane using the same assay system described in this study (see Section 2.2). However, we could not detect any GOAT activity, perhaps due to low concentrations of the enzyme in the stomach (data not shown).

2.2. *In vitro* GOAT enzymatic assay

1. The standard *in vitro* assay for the ghrelin *n*-octanoyl modification contained the following: 200 μl of 50 m*M* Tris–HCl (pH 7.4), 0.5 μ*M* rat des-acyl ghrelin, 10 μ*M* *n*-octanoyl-CoA (Sigma-Aldrich Co., St. Louis, MO), 0.1% CHAPS, and 1–5 μl enzyme solution. Figure 10.2 shows that *n*-octanoyl ghrelin was produced from the acyl donor *n*-octanoyl-CoA but not from *n*-octanoic acid. Moreover, co-incubation of both

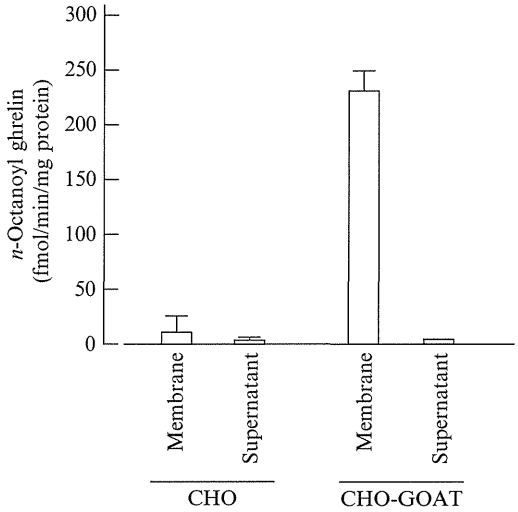

Figure 10.1 Subcellular localization of GOAT activity. Wild-type CHO and GOAT-expressing CHO (CHO-GOAT) cells were collected and separated by centrifugation at 100,000 × *g* to obtain membrane fractions. A ghrelin *n*-octanoyl modification reaction was performed using the standard assay conditions. *n*-Octanoyl ghrelin concentrations were measured using the active ghrelin ELISA kit. The results are expressed as the means ± SD ($n = 3$).

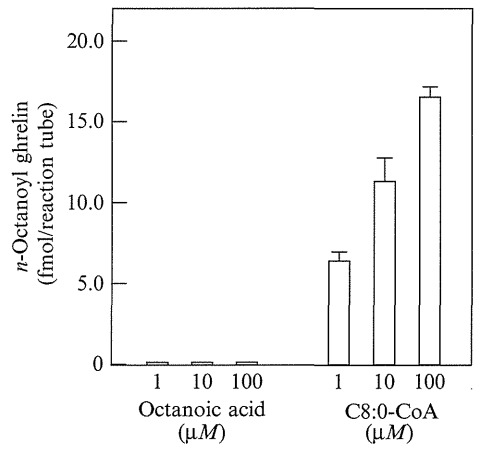

Figure 10.2 GOAT acyl donor selectivity. The production of *n*-octanoyl ghrelin was measured using the standard assay conditions with varying concentrations of *n*-octanoic acid or *n*-octanoyl-CoA as donor substrates. The results are expressed as the means ± SD ($n = 3$).

n-octanoic acid and CoA alone did not produce *n*-octanoyl ghrelin (data not shown). Thus, *n*-octanoyl-CoA was an acyl donor for ghrelin.

2. The reaction was initiated by adding the enzyme solution to the other components and incubating at 37 °C for 30 min.
3. The reaction was stopped by adding 20 µl 1 N HCl. The solution was stored at −30 °C until ghrelin concentrations were measured.

3. DETECTING THE MOLECULAR FORMS OF GHRELIN GENERATED BY *IN VITRO* GOAT ENZYMATIC ASSAYS

We used three approaches to identify the molecular forms of ghrelin produced during *in vitro* GOAT activity assays (Fig. 10.3).

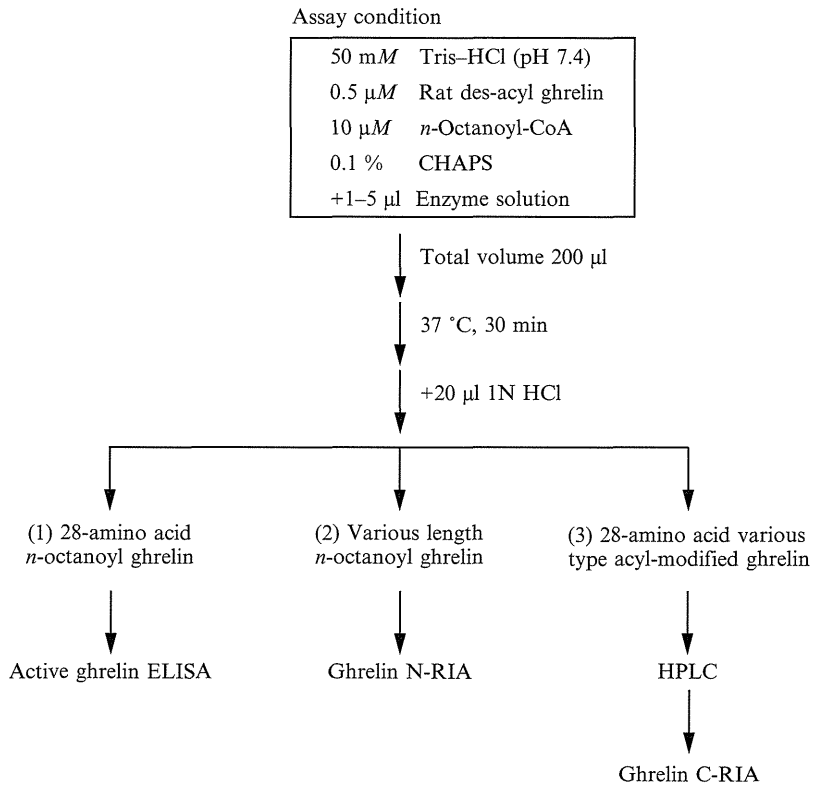

Figure 10.3 Assays to identify various molecular forms of ghrelin. Three assay systems, namely, active ghrelin ELISA, ghrelin N-RIA, and ghrelin C-RIA, were used to identify various lengths and acyl modifications of ghrelin peptides produced *in vitro*.

1. *n*-Octanoyl-modified ghrelin peptides less than 28 amino acids long were identified by a radioimmunoassay (RIA) specific to the N-terminal fragment of ghrelin (N-RIA), which detects the *n*-octanoyl moiety.
2. To analyze the various types of acyl modifications in ghrelin peptides, the assayed samples were fractionated by high-performance liquid chromatography (HPLC), and the ghrelin concentration in each fraction was detected by RIA specific to the C-terminal fragment of ghrelin (C-RIA). The various types of acyl modifications in ghrelin resulted in different retention times by HPLC; the modifications with longer acyl acids eluted earlier than those with shorter ones.
3. Full-length *n*-octanoyl ghrelin was detected by an active ghrelin ELISA kit (Mitsubishi Kagaku Iatron, Inc., Tokyo, Japan). This ELISA specifically detects *n*-octanoyl ghrelin of 28 amino acids in length.

3.1. RIA of ghrelin

1. Rabbit polyclonal antibodies were raised against N- and C-terminal rat ghrelin peptides: Gly^{1}-Lys^{11} with O-*n*-octanoylation at Ser^{3} and Gln^{13}-Arg^{28}, respectively (Hosoda et al., 2000).
2. RIA incubation mixtures contained 100 µl of either standard ghrelin or an unknown sample with 200 µl of antiserum diluted in the RIA buffer: 50 m*M* sodium phosphate buffer, pH 7.4; 0.5% BSA; 0.5% Triton X-100; 80 m*M* NaCl; 25 m*M* EDTA-2Na; 0.05% NaN_3; and 0.5% normal rabbit serum.
3. Anti-N- and C-terminal rat ghrelin antisera were used at final dilutions of $1{:}1.5 \times 10^{6}$ and $1{:}1 \times 10^{4}$, respectively.
4. After a 12-h incubation at 4 °C, 100 µl ^{125}I-labeled ligand (20,000 cpm) was added, and the incubation was continued for an additional 36 h. Then, 100 µl of anti-rabbit goat antibody was added and the samples were incubated for 24 h at 4 °C.
5. Free and bound tracers were separated by centrifugation at 3000 rpm for 40 min. The radioactivity in the pellet was quantified in a γ-counter (ARC-600, Aloka, Tokyo, Japan). All assays were performed in duplicate.
6. Both antisera exhibited complete cross-reactivity with human, mouse, and rat ghrelins. The anti-N-terminal rat ghrelin antiserum, which specifically recognizes the *n*-octanoylated portion of ghrelin, exhibited 100% cross-reactivity with rat, mouse, and human *n*-octanoyl ghrelin but did not recognize des-acyl ghrelin.

7. The anti-C-terminal rat ghrelin antiserum equally recognized both des-acyl and all acylated forms of ghrelin peptides including *n*-hexanoyl, *n*-octanoyl, *n*-decanoyl, *n*-lauroyl, *n*-myristoyl, and *n*-palmitoyl ghrelins.
8. The ED_{50} values for N- and C-terminal ghrelin RIAs were approximately 8 and 32 fmol/tube, respectively. The minimal detection levels by the N- and C-terminal RIAs were 0.25 and 1.0 fmol/tube, respectively. All samples were diluted in the RIA buffer to fit the optimal detection range (between ED_{20} and ED_{80}) for each RIA.
9. Throughout the following sections, the RIA systems using the N- and C-terminal antisera are termed N- and C-RIAs, respectively.

3.2. ELISA of ghrelin

1. An active ghrelin ELISA Kit (Mitsubishi Kagaku Iatron, Inc.) was used to specifically measure *n*-octanoyl ghrelin, and a des-acyl ghrelin ELISA Kit (Mitsubishi Kagaku Iatron, Inc.) was used to specifically assess des-acyl ghrelin.
2. Samples produced by *in vitro* GOAT enzymatic assays were directly used for the ghrelin ELISAs.

3.3. HPLC analysis of *n*-octanoyl-modified ghrelin

We analyzed the molecular forms of ghrelin in the GOAT reaction to confirm that the product was a ghrelin peptide modified by *n*-octanoyl acid.

1. The reaction products were desalted with Sep-Pak C18 cartridges (Waters, Milford, MA) that had been pre-equilibrated in 10% acetonitrile (CH_3CN)/0.1% trifluoroacetic acid (TFA). The samples were loaded onto the cartridges, which were then washed with 10% CH_3CN/0.1% TFA. The peptides were eluted with 60% CH_3CN/0.1% TFA.
2. Next, the eluate was lyophilized. Then, the peptides were resuspended in 10% CH_3CN/0.1% TFA and separated by reverse-phase HPLC (RP-HPLC) using a μBondasphere C18 column (3.9 × 150 mm; Waters) and a linear 40-min gradient of 10–60% CH_3CN in 0.1% TFA at 1 ml/min. Fractions (500 μl) were collected throughout the gradient.
3. The fractions were lyophilized and subjected to ghrelin analysis by RIA or ELISA.
4. To determine the retention times of the standard ghrelin peptides, human *n*-octanoyl ghrelin and des-acyl ghrelin, the standards were mixed with the GOAT assay solution and (without performing a reaction) the mixture was immediately desalted with a Sep-Pak C18 cartridge, lyophilized, and resuspended in 10% CH_3CN/0.1% TFA.

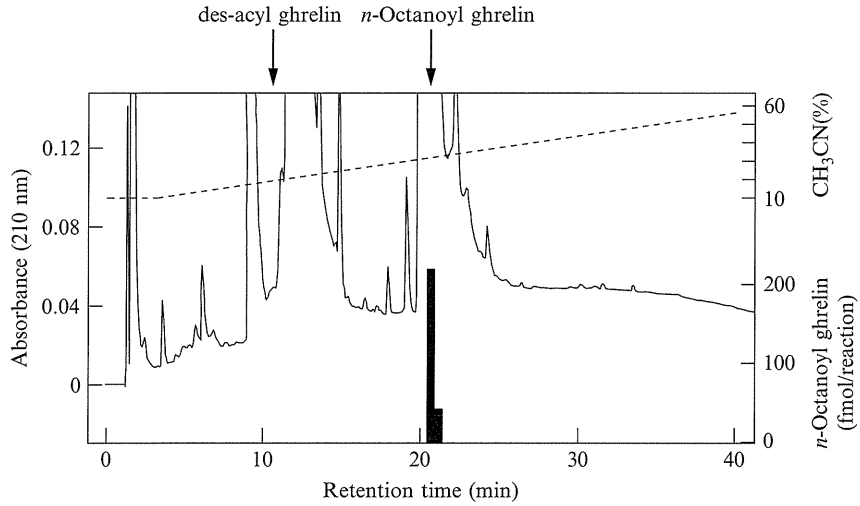

Figure 10.4 Characterization of ghrelin peptides produced by *in vitro* GOAT enzymatic reactions. RP-HPLC of GOAT reaction products was monitored by an ELISA specific for *n*-octanoyl ghrelin. The black bars indicate *n*-octanoyl ghrelin immunoreactivity. The gradient profile is indicated by the dotted line. The standard eluted positions of des-acyl ghrelin and *n*-octanoyl ghrelin are indicated by arrows.

5. Then, the peptide standards were separated by RP-HPLC and assayed by two ELISAs: the active ghrelin ELISA Kit (specific for the *n*-octanoyl peptide) and the des-acyl ghrelin ELISA Kit (specific for des-acyl peptide).
6. Standard *n*-octanoyl human ghrelin eluted in fraction 42 (at 20.5–21.0 min) and des-acyl ghrelin eluted in fraction 22 (at 10.5–11.0 min). Figure 10.4 shows the HPLC analysis of the reaction products from GOAT activity assays. Each fraction was measured by an active ghrelin ELISA. We detected immunoreactivity in fraction 42, the same elution position as the *n*-octanoyl ghrelin peptide standard. Thus, the ghrelin peptide produced by GOAT *in vitro* was identified as *n*-octanoyl ghrelin (1–28).

4. ENZYMATIC CHARACTERIZATION OF GOAT

4.1. Effect of detergents on GOAT activity

Subcellular fractionation revealed that *n*-octanoyltransferase activity partitioned with the cell membrane fraction, confirming that GOAT is a membrane-bound enzyme as suggested in the original GOAT papers (Gutierrez et al., 2008; Yang et al., 2008). We examined the effects of detergents on GOAT activity.

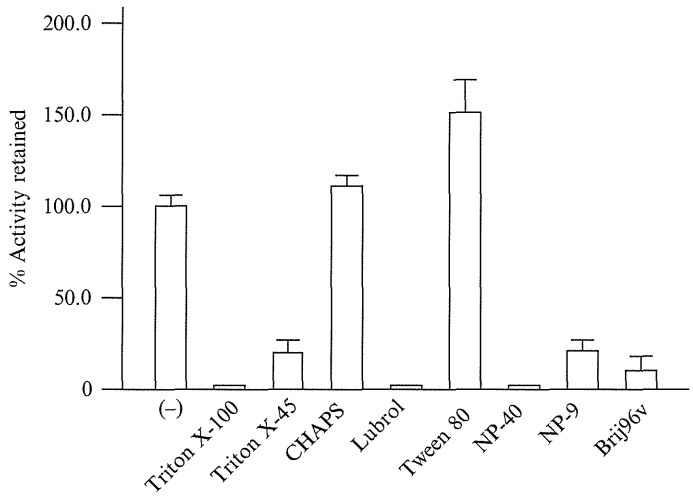

Figure 10.5 Effects of detergents on GOAT activity. Crude membranes from GOAT-expressing CHO cells were solubilized in 1% of the indicated detergent for 15 min at 37 °C. Then, the *n*-octanoyl transferase reaction was performed in the standard assay solution containing 0.1% of the indicated detergent.

1. Eight detergents were used: Triton X-100, Triton X-45, CHAPS, Lubrol, Tween 80, NP40, NP9, and Brij96v. These detergents were prepared in water to 5.0%.
2. The enzyme preparation from GOAT-expressing CHO cells was incubated in 0.1% detergent for 15 min at 37 °C. Then, the GOAT activity assay was performed according to the standard method (Section 2.2). We found that treatment of the membrane fraction with CHAPS or Tween 80 retained GOAT activity (Fig. 10.5). By contrast, treatment with the six other detergents attenuated or abolished GOAT activity. These results indicated that CHAPS and Tween 80 stabilized the conformation of GOAT and were useful for solubilization of the enzyme.

4.2. Exploration of GOAT acyl donors

To investigate whether GOAT utilizes only *n*-octanoyl-CoA as an acyl donor, we assessed the ability of recombinant GOAT to acylate ghrelin using a variety of *n*-acyl-CoAs, including *n*-hexanoyl-, *n*-decanoyl-, *n*-palmitoyl-, and *n*-myristoyl-CoA (Ohgusu et al., 2009). The reaction conditions were the same as for the standard reaction mixture except for the substitution of *n*-acyl-CoA substrates in place of *n*-octanoyl-CoA. The reaction products were subjected to HPLC analyses to confirm the molecular structure by comparison

with synthetic standard peptides. To monitor the retention time of acyl-modified ghrelins, we used C-RIA, which recognizes the C-terminal portion of the ghrelin peptide and is not affected by acyl modifications.

1. Fatty acid-CoAs used for the acyl donor studies were purchased from Sigma-Aldrich Co.. These fatty acid-CoAs were used at the standard assay concentration of 10 μ*M*.
2. The reaction products were desalted with Sep-Pak C18 cartridges and subjected to RP-HPLC after evaporation of acetonitrile and resuspension in 10% CH_3CN/0.1% TFA. A 40-min linear gradient of 10–60% CH_3CN in 0.1% TFA was used at 1 ml/min. Fractions (500 μl) were collected throughout the gradient.
3. The fractions were lyophilized and analyzed by anti-ghrelin C-RIA. Ghrelin immunoreactive fractions were compared with the standard elution times of synthetic *n*-acyl-modified ghrelins. We found that, in addition to *n*-octanoyl CoA, GOAT modified the des-acyl ghrelin peptide with other medium-chain acyl acids, such as *n*-hexanoyl-CoA (Fig. 10.6A) and *n*-decanoyl-CoA (Fig. 10.6B). By contrast, long-chain fatty acids were not used as acyl donors. Next, we conducted kinetic studies using des-acyl ghrelin and three medium-chain acyl-CoAs as the donor substrates: *n*-hexanoyl-, *n*-octanoyl-, and *n*-decanoyl-CoA (Fig. 10.6C and D). Increasing the acyl-CoA concentrations resulted in increasing GOAT activity. The order of substrate preference as evaluated by V_{max}/K_m was *n*-hexanoyl-CoA > *n*-octanoyl-CoA > *n*-decanoyl-CoA. The K_m values of *n*-hexanoyl-CoA and *n*-octanoyl-CoA were 294 and 13.6 μ*M*, respectively. We could not calculate the K_m values of *n*-decanoyl-CoA because the concentration of the produced *n*-decanoyl ghrelin was very low.

4.3. Substrate specificity of GOAT for ghrelin peptides

We examined the peptide substrate specificity of GOAT (Ohgusu et al., 2009). Synthetic peptide substrates were derived from the N-terminal sequence of mammalian ghrelin. The length of these substrates (four to eight amino acids) was shorter than that of des-acyl ghrelin, and the C-terminus of the peptide substrates had an α-amide structure. N-RIA was used for the detection of *n*-octanoyl-modified peptides.

1. Short (four to eight amino acids) synthetic ghrelin peptides and *n*-octanoyl-CoA were used as the peptide and acyl donor substrates, respectively. The synthetic peptides were GSSF-NH_2, GSSFL-NH_2, GSSFLK-NH_2, GSSFLSP-NH_2, and GSSFLSPK-NH_2.

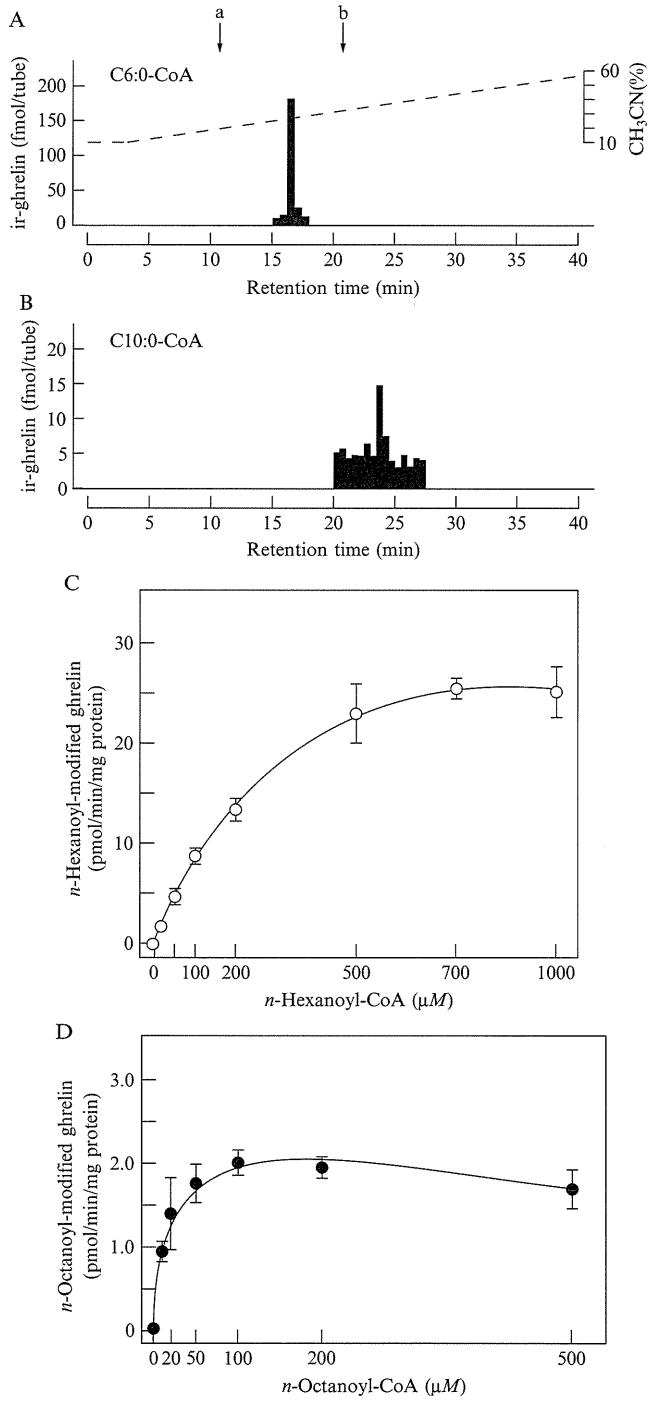
A
a
b
C6:0-CoA
ir-ghrelin (fmol/tube)
200
150
100
50
0
60
10
CH_3CN(%)
0 5 10 15 20 25 30 35 40
Retention time (min)
B
C10:0-CoA
ir-ghrelin (fmol/tube)
20
15
10
5
0
0 5 10 15 20 25 30 35 40
Retention time (min)
C
n-Hexanoyl-modified ghrelin (pmol/min/mg protein)
30
20
10
0
0 100 200 500 700 1000
n-Hexanoyl-CoA (μ*M*)
D
n-Octanoyl-modified ghrelin (pmol/min/mg protein)
3.0
2.0
1.0
0
0 20 50 100 200 500
n-Octanoyl-CoA (μ*M*)

2. The reaction products were directly subjected to RP-HPLC analysis using a 40-min linear gradient of 10–60% CH_3CN in 0.1% TFA at 1 ml/min. Fractions (500 μl) were collected throughout the gradient.
3. Fractions were lyophilized, reconstituted in RIA buffer, and analyzed by N-RIA. Figure 10.7 shows the HPLC retention times of the five synthetic ghrelin-derived substrates. The retention times of the reaction products were delayed for all of the peptide substrates assayed. The retention times were as follows: 23.5–24.5 min, GSSF-NH_2; 26.0–26.5 min, GSSFL-NH_2; 23.0–23.5 min, GSSFLK-NH_2; 25.0–25.5 min, GSSFLSP-NH_2; and 23.5–24.0 min, GSSFLSPK-NH_2. Moreover, the synthetic *n*-octanoyl-modified peptide GSS(C8:0)FLSPK-NH_2 had the same retention time as that of the GOAT-reacted GSSFLSPK-NH_2 product (data not shown). These results indicated that these five peptides served as GOAT substrates that were modified by *n*-octanoic acid. Furthermore, peptides as short as four amino acids were sufficient to serve as GOAT substrates.

4.4. Optimal temperature and pH for GOAT activity

The optimal reaction temperature was from 37 to 50 °C (Fig. 10.8A). GOAT activity was retained at 55 °C but was abolished above 60 °C. The specific activity of GOAT was determined over a range of pH values (Fig. 10.8B) using the following buffers: 50 m*M* MES (pH 5–7), Tris–HCl (pH 7.5–8.5), and $NaHCO_3$ (pH 9–10). The optimal pH for maximal specific activity was pH 7.0–7.5. The specific activity dropped off rapidly below pH 6.5 and above pH 8.5.

4.5. Effects of cations on GOAT activity

The effects of various cations on GOAT activity were compared (Fig. 10.9). Recombinant GOAT was activated by low concentrations but inhibited by high concentrations of Mg^{2+} and Ca^{2+}. By contrast, Fe^{3+} and Cu^{2+}

Figure 10.6 Acyl-CoA specificity of GOAT. The acyl-CoA specificity of GOAT toward (A) *n*-hexanoyl-CoA (C6:0) and (B) *n*-decanoyl-CoA (C10:0) was analyzed by incubating 0.5 μ*M* rat des-acyl ghrelin in the presence of 1 μl enzyme solution. Two reactions for each acyl-CoA were performed; these reactions were pooled for HPLC analyses. The reaction products were subjected to HPLC, and each fraction was assayed for immunoreactive ghrelin by ghrelin C-RIA. The arrows indicate the eluted positions of (a) des-acyl ghrelin and (b) *n*-octanoyl ghrelin. (C and D) Kinetic studies of recombinant GOAT. GOAT assays were performed by incubating increasing concentrations of (C) *n*-hexanoyl-CoA (C6:0), (D) *n*-octanoyl-CoA (C8:0), and (not shown) *n*-decanoyl-CoA (C10:0) under the same assay conditions. The concentrations of acylated ghrelin products were measured using ghrelin C-RIA after HPLC. The K_m values were calculated from these results.

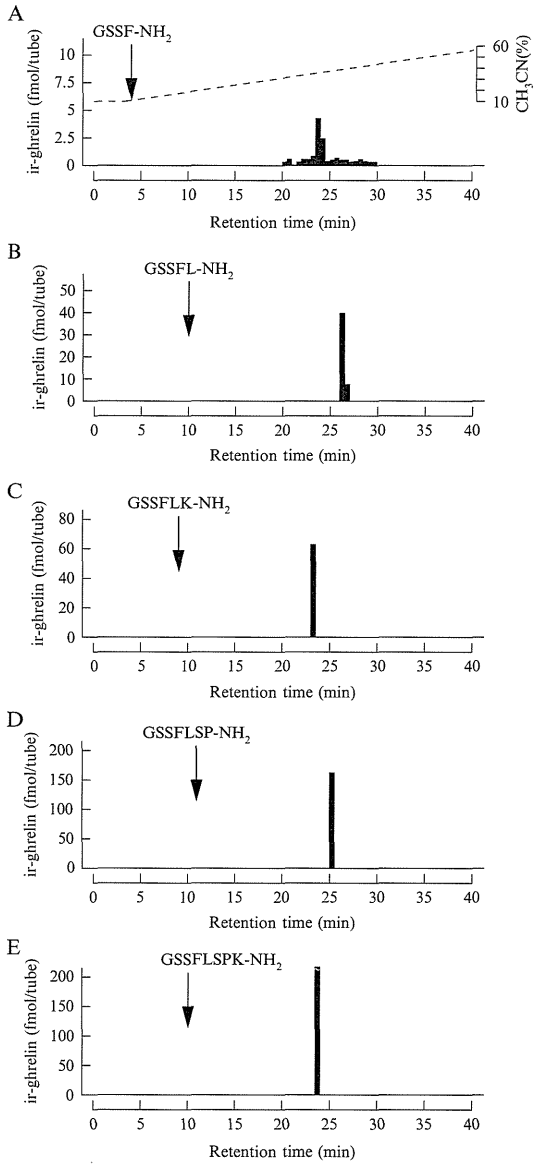

Figure 10.7 Analysis of GOAT substrate specificity. HPLC analyses of GOAT reaction products when (A) GSSF-NH_2, (B) GSSFL-NH_2, (C) GSSFLK-NH_2, (D) GSSFLSP-NH_2, and (E) GSSFLSPK-NH_2 were used as substrates. Reaction products were subjected to HPLC and each fraction was assayed for immunoreactive *n*-octanoyl ghrelin by N-RIA. The eluted positions of peptide substrates are indicated by arrows.

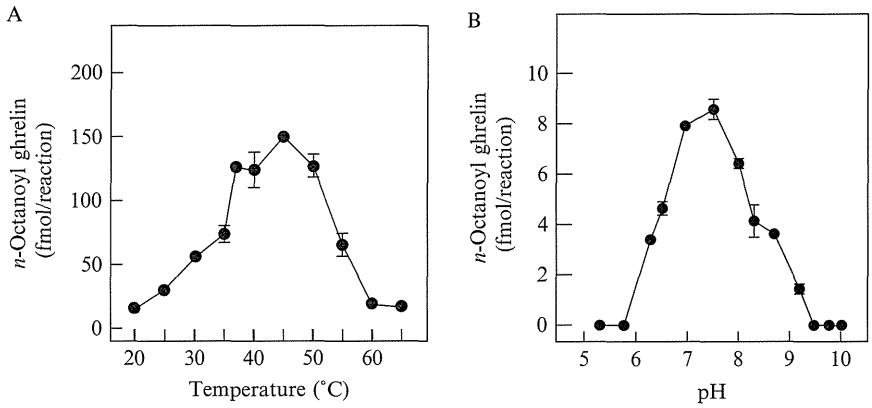

Figure 10.8 Optimal temperature and pH for GOAT activity. *n*-Octanoyl ghrelin concentrations were measured by the active ghrelin ELISA kit. Results are expressed as the mean ± SD ($n = 3$). (A) Temperature dependence of GOAT activity. (B) pH dependence of GOAT activity.

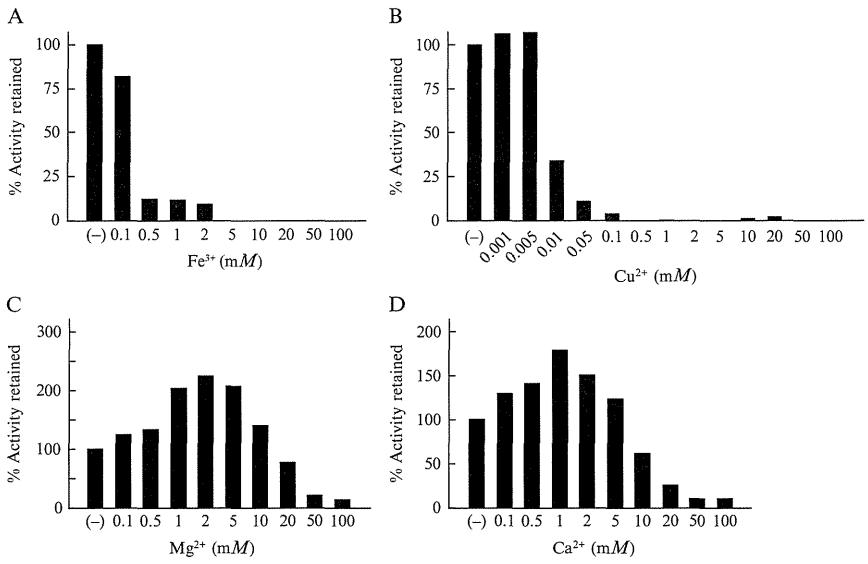

Figure 10.9 Effects of cations on GOAT activity. Enzymatic activity was measured using standard assay conditions with the addition of cations. The cations used were (A) $FeCl_3$, (B) $CuCl_2$, (C) $MgCl_2$, and (D) $CaCl_2$. Activity is expressed as the percent activity retained after cation treatment as compared to standard assay conditions. Data represent the average of two independent experiments.